

Influence of Ca/P Concentration on Hydroxyapatite (HAp) from Asian Moon Scallop Shell (*Amusium Pleuronectes*)

Firda Yanuar Syafaat and Yusril Yusuf*

Department of Physics, Faculty of Mathematics and Natural Science, Universitas Gadjah Mada, Sekip Utara, Yogyakarta 55281, Indonesia.

Received 18 May 2018, Revised 30 August 2018, Accepted 13 March 2019

ABSTRACT

Hydroxyapatite (HAp) derived from the scallop shell was successfully prepared using a precipitation method and varying the Ca/P concentration. Scallop shells were calcined at 1000°C to produce CaO. The precursors were a Ca(OH)₂ suspension and an H₃PO₄ solution, and the HAp was synthesized by mixing the two precursors and calcining at 1050°C. The aim of this study was to investigate the effect of Ca/P concentration. Samples were characterized by XRD, SEM-EDX, and FTIR. The XRD patterns indicated an increase in crystallinity with increasing Ca/P concentration ratio. The lattice parameter and the density values of the 0.5/0.3 sample approached the theoretical value. The crystallite sizes of HAp powders ranged from 79.750 ± 0.066 to 90.932 ± 0.071 nm. The Ca/P ratios of 0.5/0.3 and 1/0.6 were 1.68 and 1.67. The FTIR spectra confirmed the presence of functional groups of PO₄³⁻ and OH.

Keywords: Hydroxyapatite, Scallop Shell, Precipitation, Ca/P Concentration.

1. INTRODUCTION

The scallop, *Amusium pleuronectes*, is a shellfish species of the Pectinidae family endemic to tropical seabeds [1]. It is an abundant species that is easy to find in many places in Indonesia. The shell of this scallop contains 96.15% calcium oxide (CaO) [2], making it an excellent source of calcium for hydroxyapatite (HAp) synthesis.

Hydroxyapatite (chemical formula Ca₁₀(PO₄)₆OH₂) is a calcium-phosphate mineral phase with a Ca/P ratio of 1.67 [3,4] that shows good bioactivity, biocompatibility, and osteoconductive properties [5]. Their bioactivity, biocompatibility, and osteoconductivity are demonstrated by the ability to stimulate new bone ingrowth around implants, to perform an appropriate response, and to provide a correct scaffold for bone formation [4-6].

HAp can be synthesized by several methods that can involve precipitation [7], hydrothermal [8], sol-gel [9], or solid-state reactions [10]. The method chosen in the present research was a precipitation method, as it is easily performed, requires no special equipment, and can be conducted at low temperatures [10,11]. Several factors affect the process of HAp synthesis through this method, including the reactants involved in the synthesis process, their concentrations, the pH of the reaction solution, and the calcination temperature [12].

HAp is not formed directly; rather, its synthesis occurs through several phases involving previously formed compounds, such as dicalcium phosphate dihydrate (DKFD) and octacalcium

*Corresponding Author: yusril@ugm.ac.id

phosphate (OKF). Conversion of DFKD to OKF takes about 60 s, whereas conversion of OKF to HAp takes at least 100 hours. According to Czernuszka, this long formation time is due to the concentration of calcium and phosphate ions (2.4 mM) and the pH (pH 7.4) of the reaction mixture. The higher the initial concentration of calcium and phosphate ion, the higher of crystallinity and the faster of forming the time of HAp [13]. Therefore, knowledge of the optimum ratios of Ca/P is needed to obtain HAp with good purity and the desired properties. The aim of the present study was to investigate the effects of varying the Ca/P concentration ratio on HAp synthesized by the precipitation method.

2. METHODS

2.1 Preparation of CaO

The raw material used for the manufacture of CaO was scallop shells. The shells were cleaned and then dried in an oven at 100°C for 1 hour. The shells were smoothed with a ball mill and then calcined at 1000°C for 5 hours in a furnace.

2.2 Synthesis of Hap

Ca(OH)₂ and H₃PO₄ were used a calcium and phosphorous precursors, respectively. Ca(OH)₂ suspension was obtained from the reaction between CaO of the scallop shell and H₂O, as seen in Equation 1.



The starting concentration of Ca(OH)₂ was 0,5 M, 1 M, and 1,67 M, whereas H₃PO₄ was added dropwise into the Ca(OH)₂ suspension and the resultant mixture was heated at 60°C. The NH₄OH solution was added to the mixture of Ca(OH)₂ and H₃PO₄ if the pH was less than 9. The solution was allowed to the precipitate for 24 hours at room temperature. After this, the solution was stirred for 30 minutes. The resultant of stirring was filtered and dried at 100°C. The dried powder was calcined at 1050°C.

2.3 Characterization of Hap

The HAp was characterized by X-ray diffractometry (XRD), Fourier transform infrared (FTIR) spectroscopy, scanning electron microscopy (SEM), and energy dispersive X-ray (EDX) spectroscopy. XRD was used to determine the crystalline phases, the lattice parameter, the density, and the crystallite size of the HAp. The obtained crystalline phases were compared against the Joint Committee on Powder Diffraction Standards (JCPDS). FTIR was used for the identification of functional groups and interactions between molecules. SEM was used to view the morphology of the particles, and EDX was used to determine the mass percentage of the elements to obtain the Ca/P ratio of the HAp.

3. RESULTS AND DISCUSSION

3.1 Calcination of a Scallop Shell

Table 1 The mass efficiency of a calcined scallop shell

Mass (gr)		Efficiency
Before calcination	After calcination	
55.215	31.464	56.98

The efficiency of shell mass conversion after calcination is shown in Table 1. Mass Conversion in Table 1 indicates a reduction in shell mass after calcination. This reduction occurs because the shell undergoes decomposition that caused by the heat[14]. Water is physically adsorbed at 90–120°C, the decomposition of magnesium carbonate ($MgCO_3$) and hydrocarbon combustion occurs at 250–400°C, the decomposition of $CaCO_3$ occurs at 750–850°C, and the decomposition of $CaCO_3$ to CaO occurs at 1000°C [15]. The reaction of the calcination process is shown in Equation 2.



The reaction in Equation 2 is known as a thermal decomposition reaction. the atom moves rapidly and causes the chemical bond of $CaCO_3$ to decompose into CaO and CO_2 when the compound is heated.

3.2 Characterization of HAp from a Scallop Shell

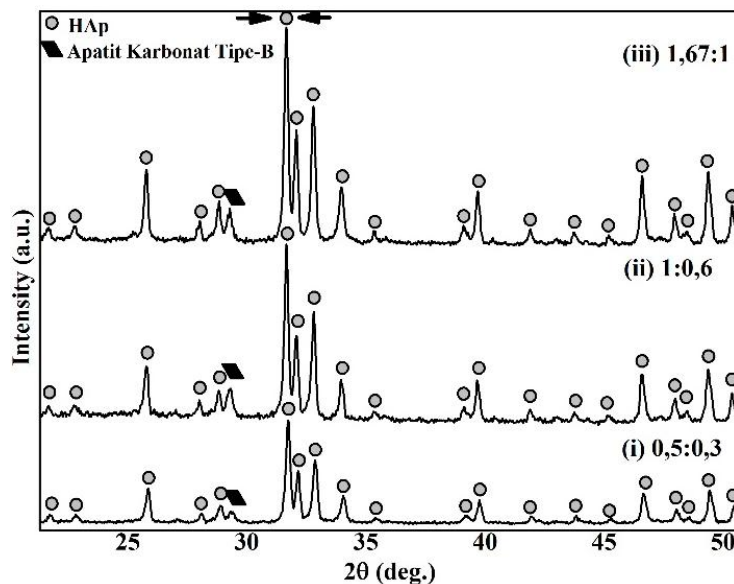


Figure 1. XRD pattern of HAp with Ca/P concentration (i) 0.5:0.3, (ii) 1:0.6, and (iii) 1.67:1.

The crystal phase was identified by XRD, and the resulting peak pattern was compared to the JCPDS standard reference for HAp (JCPDS 9-432). The XRD pattern for the HAp sample, after sintering at 1050°C, is shown in Figure 1. All the samples showed peaks corresponding to HAp. However, the XRD pattern shows the presence of B-type carbonate apatite, and this peak increases as the Ca/P concentration ratio increases. In general, the carbonate apatite in HAp exhibits a higher resorbability and better osteoconductive properties than does pure HAp [16]. However, the high content of B-type carbonate apatite causes too much absorption in the human body and degrades the strength of artificial bone replacements [17].

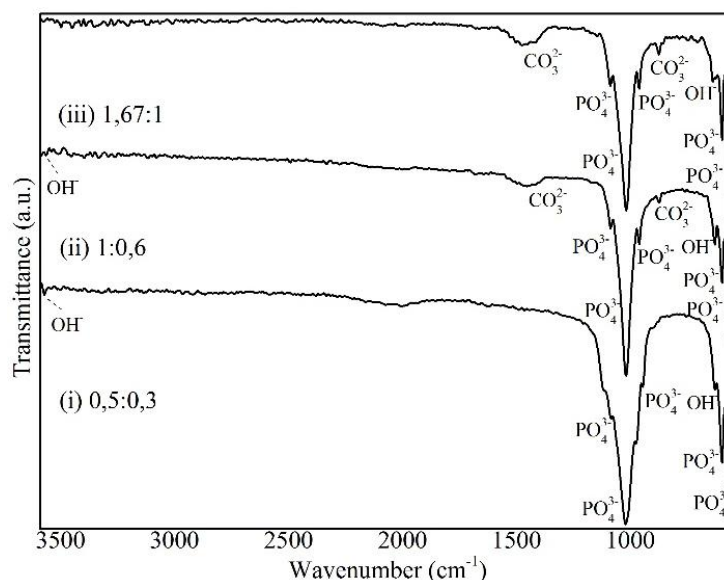
The crystallinity of HAp increases as the concentration ratio increases, and this increased crystallinity is characterized by increasing diffraction peaks[18], as indicated in Figure 1, where the HAp peak becomes sharper and narrower. Syafaat and Yusuf also confirmed that HAp crystallinity is better for HAp with a high concentration ratio than with a low concentration ratio [19].

Table 2 Lattice parameter, density, crystallite size, and Ca/P ratio of Hap

Sample	Lattice Parameter		Density (gr/cm ³)	Crystallite size (nm)	Ca/P ratio
	a (Å)	c (Å)			
0.5/0.3	9.413	6.878	3.17	79.750 ± 0.066	1.68
1/0.6	9.361	6.841	3.22	87.198 ± 0.091	1.67
1.67/1	9.298	6.792	3.29	90.932 ± 0.071	2.08

HAp has a Ca/P ratio of 1.67 and a density value of 3.16 (gr/cm³) [20]. The synthesized HAp has a hexagonal crystal structure with a symmetry distance between the P6₃/m groups and the lattice parameters of $a=b=9.418$ Å, $c=6.881$ Å, and $\gamma=120$ [21]. As shown in Table 2, the value of the lattice parameters and the density that approximates the theoretical result is the HAp sample with the concentration ratio of 0.5/0.3. The corresponding Ca/P ratio, in theory, is the Ca/P ratio of HAp with a concentration of 0.5/0.3 and 1/0.6.

Table 2 shows that the lattice parameters a and b become smaller as the concentration ratio increases. This shrinkage will occur because the porosity of the surface becomes smoother [22]. By contrast, the density and crystallite size of the HAp increases when the Ca/P concentration ratio increases.

**Figure 2.** FTIR spectrum of HAp at Ca/P concentration (i) 0.5:0.3, (ii) 1:0.6, and (iii) 1.67:1.

The functional groups and interactions between molecules were identified by FTIR. The FTIR spectrum of the HAp sample after sintering at 1050°C is shown in Figure 2. According to Mobasherpour *et al.*, HAp has main peaks of PO₄³⁻ and OH⁻ [23]. Therefore, the final formed sample was confirmed as HAp with Ca/P concentration of 0.5/0.3. A sample with a Ca/P concentration ratio of 1/0.6 indicates the presence of a functional group of CO₃²⁻. The presence of CO₃²⁻ is due to the replacement of the functional group of PO₄³⁻ with the functional group of CO₃²⁻ [24].

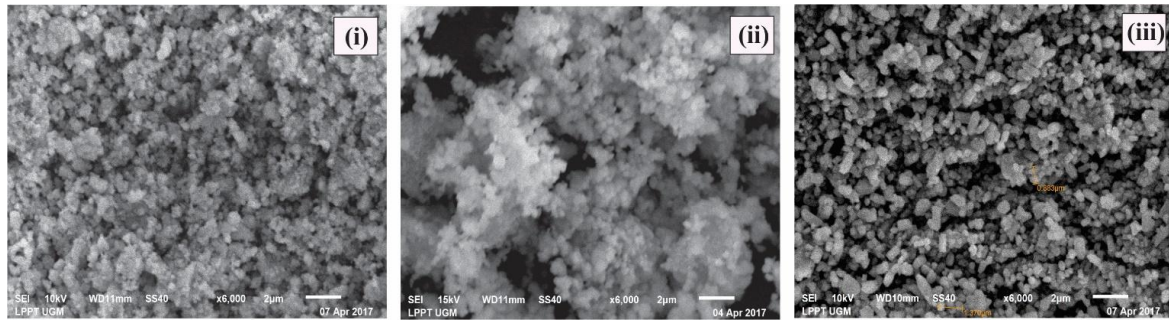


Figure 3. SEM of HAp at Ca/P concentration (i) 0.5:0.3, (ii) 1:0.6, and (iii) 1.67:1.

The morphology of the HAp sample after sintering at 1050°C, as determined by SEM, is shown in Figure 3. The SEM images for HAp with Ca/P concentration ratios of 0.5/0.3 and 1.67/1 indicate that the HAp particles have a uniform size and a regular shape. By contrast, the HAp with a Ca/P concentration ratio of 1/0.6 shows the presence of spherical agglomerates formed by small round grains. morphology of particles in HAp with a low ratio of Ca/P concentration (0.5/0.3 and 1/0.6) is a spherical shape as opposed to the morphology of particles in HAP with a high of Ca/P concentrations is an elongated shape.

4. CONCLUSION

The HAp synthesized with varying concentrations of the reactants were characterized by XRD, FTIR, and SEM-EDX. The Ca/P concentration ratio affected the final crystallinity, lattice parameter, density, crystallite size, Ca/P ratio, size, and shape of the HAp, as well as its functional groups. A higher concentration of Ca/P resulted in higher HAp crystallinity, density, and crystal size. The lattice parameters of HAp show shrinkage when the Ca/P concentration ratio increases.

ACKNOWLEDGEMENT

The authors gratefully acknowledge the financial support in this research provided by the Indonesian Ministry of Research, Technology, and Higher Education through PTUPT (2740/UN1.DITLIT/DIT-LIT/LT/2019). The authors also thank LPPT UGM for technical assistance.

REFERENCES

- [1] A. Nurdina, "Preparasi dan karakterisasi limbah biomaterial cangkang kerang simping (*Amusium pleuronectes*) dari daerah teluk lampung sebagai bahan dasar keramik," Bachelor thesis, Dept. Physics, Universitas Lampung, Lampung, Indonesia, (2016).
- [2] W. Suryaputra, I. Winata, N. Indraswati & S. Ismadji, "Waste capiz (*Amusium cristatum*) shell as a new heterogeneous catalyst for biodiesel production," *Renew. Energy* **50** (2013) 795–799.
- [3] B. R. Sunil & M. Jagannatham, "Producing hydroxyapatite from fish bones by heat treatment," *Mater. Lett.* **185** (2016) 411–414.
- [4] R. Solihat, "Hydrothermal Synthesis of Hydroxyapatite From Eggshell : Xrd , Ftir and Sem-Edxa Characterization," Bachelor thesis, Dept. Physics, Bogor Agricultural University, Bogor, Indonesia, (2008).
- [5] S. Jain, "Processing of hydroxyapatite by biomimetic process," Bachelor thesis, Dept.

- Ceramic Engineering, National Institute of Technology Rourkela, Odisha, India, (2010).
- [6] K. S. Vecchio, X. Zhang, J. B. Massie, M. Wang & C. W. Kim, "Conversion of bulk seashells to biocompatible hydroxyapatite for bone implants," *Acta Biomater.* **3**, 6 (2007) 910–918.
- [7] S. Rujitanapanich, P. Kumpapan & P. Wanjanoi, "Synthesis of hydroxyapatite from oyster shell via precipitation," *Energy Procedia* **56**, C (2014) 112–117.
- [8] M. Kamitakahara, T. Nagamori, T. Yokoi & K. Ioku, "Carbonate-containing hydroxyapatite synthesized by the hydrothermal treatment of different calcium carbonates in a phosphate-containing solution," *J. Asian Ceram. Soc.* **3**, 3 (2015) 287–291.
- [9] C. G. Vázquez, C. P. Barba & N. Munguía, "Stoichiometric hydroxyapatite obtained by precipitation and sol gel processes," *Rev. Mex. Fis.* **51**, 3 (2005) 284–293.
- [10] N. Monmaturapoj & C. Yatongchai, "Effect of sintering on microstructure and properties of hydroxyapatite produced by different synthesizing methods," *J. Met. Mater. Miner.* **20**, 2, (2010) 53–61.
- [11] A. Wang, D. Liu, H. Yin, H. Wu, Y. Wada & M. Ren, "Size-controlled synthesis of hydroxyapatite nanorods by chemical precipitation in the presence of organic modifiers," *J. Mat. Sci. Eng. C.* **27** (2007) 865–869.
- [12] N. Angelescu, D. Ungureanu & F. Anghelina, "Synthesis and characterization of hydroxyapatite bioceramic," **462** (2011) 458–462.
- [13] Balgies, "Sintesis dan Karakterisasi Hidroksiapatit dari Cangkang Kerang Ranga," Bachelor thesis, Dept. Physics, Bogor Agricultural University, Bogor, Indonesia, (2011).
- [14] M. Sari & Y. Yusuf, "Synthesis and characterization of hydroxyapatite based on green mussel shells (*Perna viridis*) with calcination temperature variation using the precipitation method," *IJNeaM* **11** (2018) 357-370.
- [15] A. Singh & K. M. Purohit, "Chemical synthesis, characterization and bioactivity valuation of hydroxyapatite prepared from garden snail (*Helix aspersa*)," *J Bioproses Biotechniq* **1**, 1.
- [16] S. Paul, A. Pal, A. Roy & S. Bodhak, "Effect of trace elements on the sintering effect of fish scale derived hydroxyapatite and its bioactivity," **43** (2017) 15678–15684.
- [17] Y. Sung, J. Lee & J. Yang, "Crystallization and sintering characteristics of chemically precipitated hydroxyapatite nanopowder," **262** (2004) 467–472.
- [18] Y. Rizkayanti & Y. Yusuf, "Effect of Temperature on Synthesis Hydroxyapatite from Cockle Shell (*Anadara granosa*)," to be published in *The International Journal of Nanoelectronics and Materials*, (2018).
- [19] F. Y. Syafaat & Y. Yusuf, "Effect of Ca:P Concentration Temperature on Hydroxyapatite (HAp) Powders From Quail Eggshell (*Coturnix coturnix*)," to be published in *The International Journal of Nanoelectronics and Materials*, (2018).
- [20] T. Laonapakul, "Synthesis of hydroxyapatite from biogenic wastes," *Kku Eng. J.* **41**, 4 (2015) 537–545.
- [21] Suryadi, "Sintesis dan karakterisasi biomaterial hidroksiapatit dengan proses pengendapan kimia basah," M.S. Thesis, Dept. Metallurgical and Materials Engineering, Universitas Indonesia, Depok, Indonesia, (2011).
- [22] F. Y. Syafaat, "Synthesis and Characterization of Hydroxyapatite Based on CapizShell and Quail Eggshell with Variation of Ca:P Concentration and Sintering Hysroxyapatite," M.Sc. Thesis, Universitas Gadjah Mada, Indonesia, (2017).
- [23] I. Mobasherpour, M. S. Heshajin, A. Kazemzadeh & M. Zakeri, "Synthesis of nanocrystalline hydroxyapatite by using precipitation method," **430** (2007) 330–333.
- [24] S. Wu, H. Hsu, S. Hsu, Y. Chang & W. Ho, "Effects of heat treatment on the synthesis of hydroxyapatite from eggshell powders," *Ceram. Int.* **41**, 9 (2015) 10718–10724.